A *Fusarium graminearum* effector protein subverts plant immunity by targeting the TaRPM1–TaHSA32 regulatory axis

Supplementary Figure

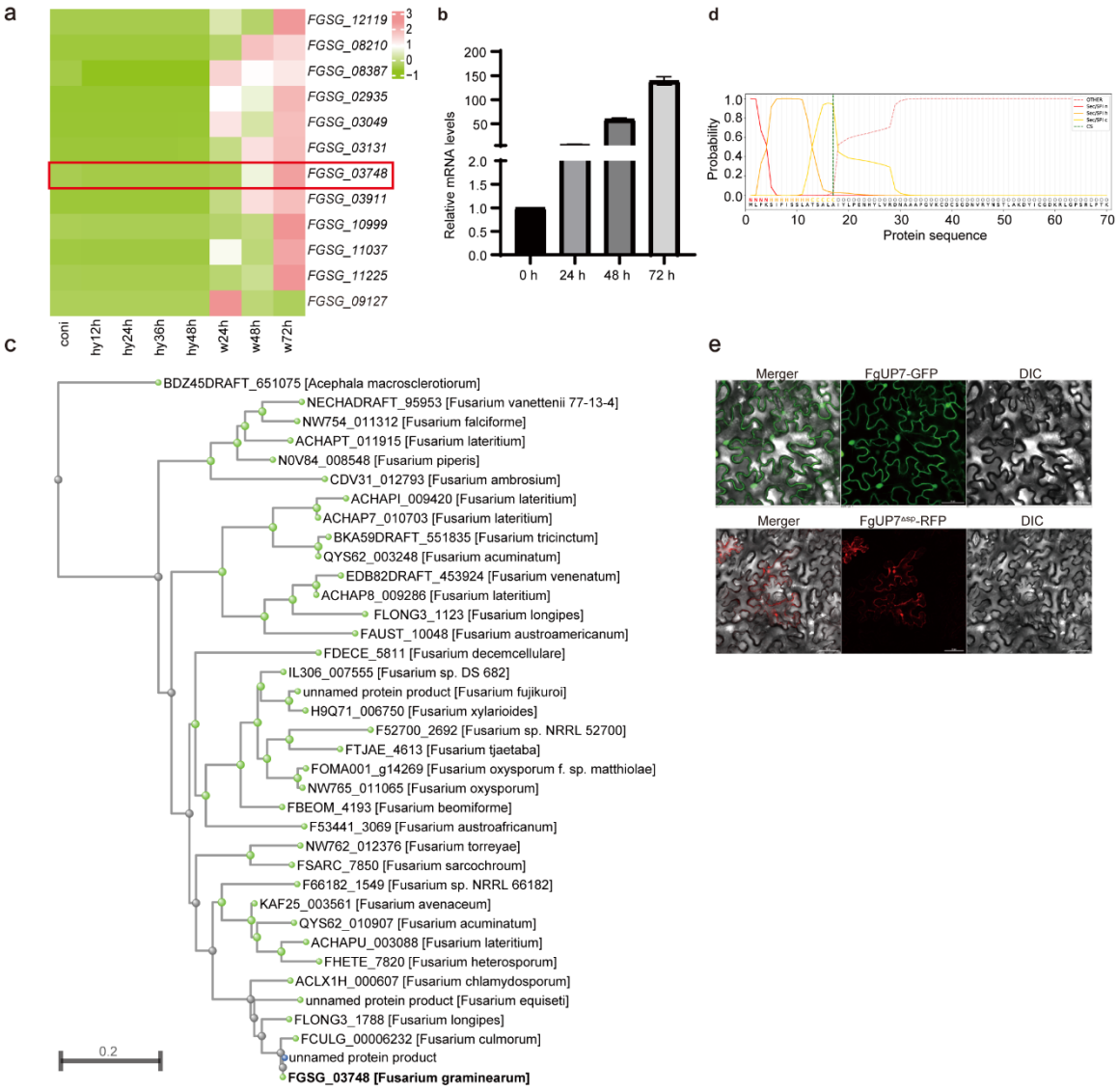

Supplementary Fig. 1 Identification of putative candidate effectors from *F. graminearum*.

(a) The expression of *F. graminearum* effectors candidates at different infection time points (12, 24, 48, and 72 hpi). The mean expression levels (n=3), presented as log_2-transformed transcripts per million (TPM) values, were used to generate a heatmap using TBtools.

(b) Transcript levels of *FgUP7* during *F. graminearum* infection of wheat heads (0, 24, 48 and 72 hpi). *FgActin* was used as the internal reference gene. Standard deviation and mean fold changes from three biological replicates. The asterisk indicates a significant difference compared with the sample at 0 hpi (one-tailed Student's t test).

(c) Phylogenetic analysis of FgUP7 orthologs. The phylogenetic tree was constructed with MEGA7 using neighbor-joining methods. The scale bar corresponds to a genetic distance of 0.02.

(d) The signal peptide of FgUP7 was predicted by Signa-IP 6.0.

(e) The localization of FgUP7 and FgUP7$^{\Delta SP}$ was achieved by infecting *N. benthamiana* leaves with *A. tumefaciens* strains containing FgUP7 and FgUP7$^{\Delta SP}$. Fluorescence signals were detected at 48 hpi. Bar, 50 μm.

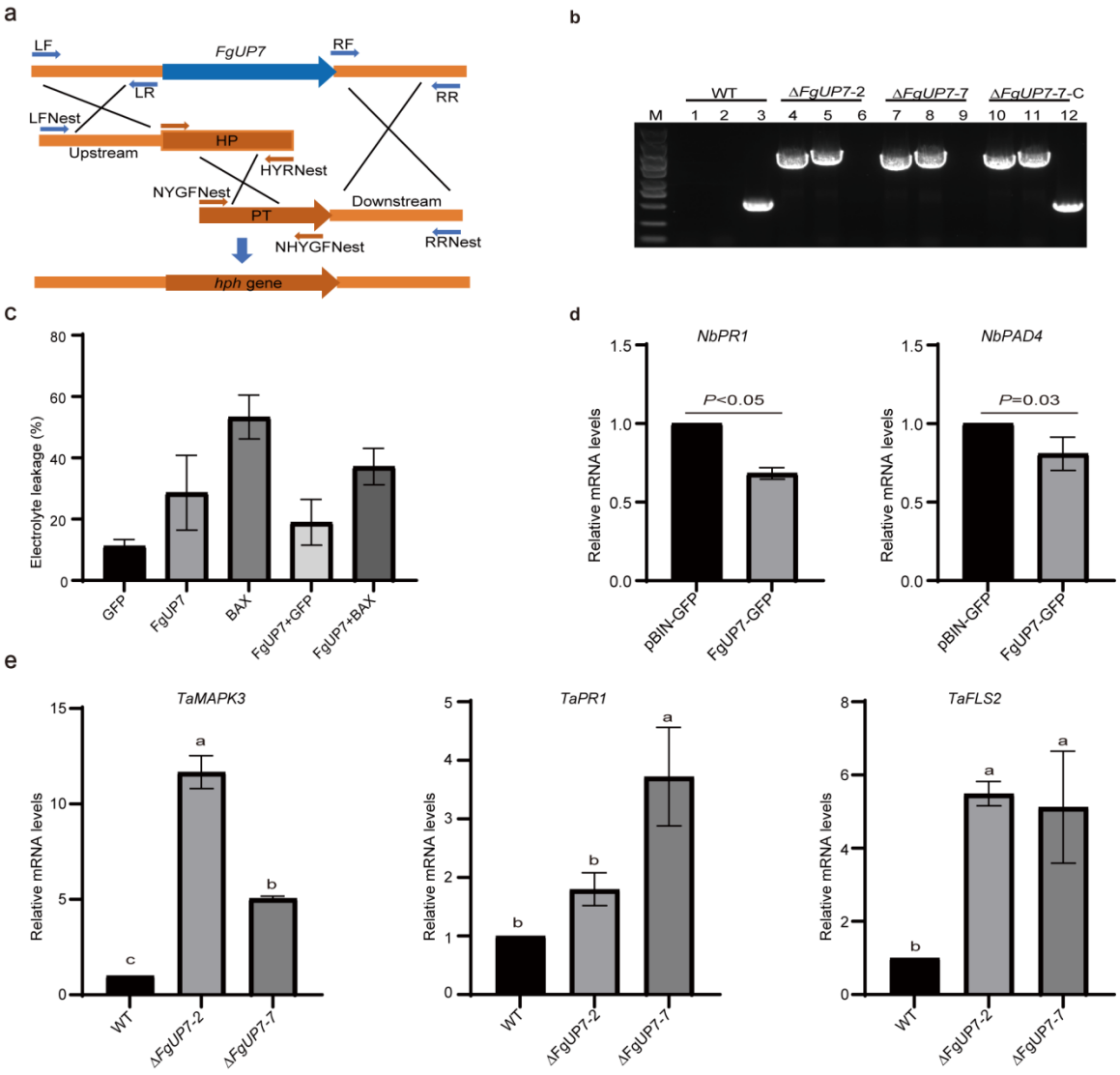

Supplementary Fig. 2 Confirmation of *F. graminearum* effector candidate (FgUP7) mutants and the plant basal defense gene expression.

(a) Schematic diagram showing the construction of homologous recombination of the gene knockout box.

(b) (1) upstream region of *FgUP7* was determined using LF/HYGR primers in lanes 1, 4, 7, and 10; (2) downstream sequence of *FgUP7* was detected using HYGF/RR primers in lanes 2, 5, 8, and 11; (3) partial sequence of *FgUP7* was amplified using UP7F/UP7R primers in lanes 3, 6, 9, and 12; M: DL5000 marker.

(c) Suppression of Bax-induced ion leakage by transiently expressed FgUP7 in leaves of 4-wk–old *N. benthamiana* plants.

(d) The expression levels of *NbPR1* and *NbPAD4* were analyzed by RT–qPCR after transient expression of GFP (control) and FgUP7 in leaves of *N. benthamiana* plants. The values are represented by means ± SD from three biological replicates (one-tailed Student's *t*-test).

(e) Relative expression levels of *TaMAPK3*, *TaPR1* and *TaFLS2* in WT and FgUP7 deletion mutant during wheat head infection. The values are represented by means ± SD from three biological replicates (one-way ANOVA test).

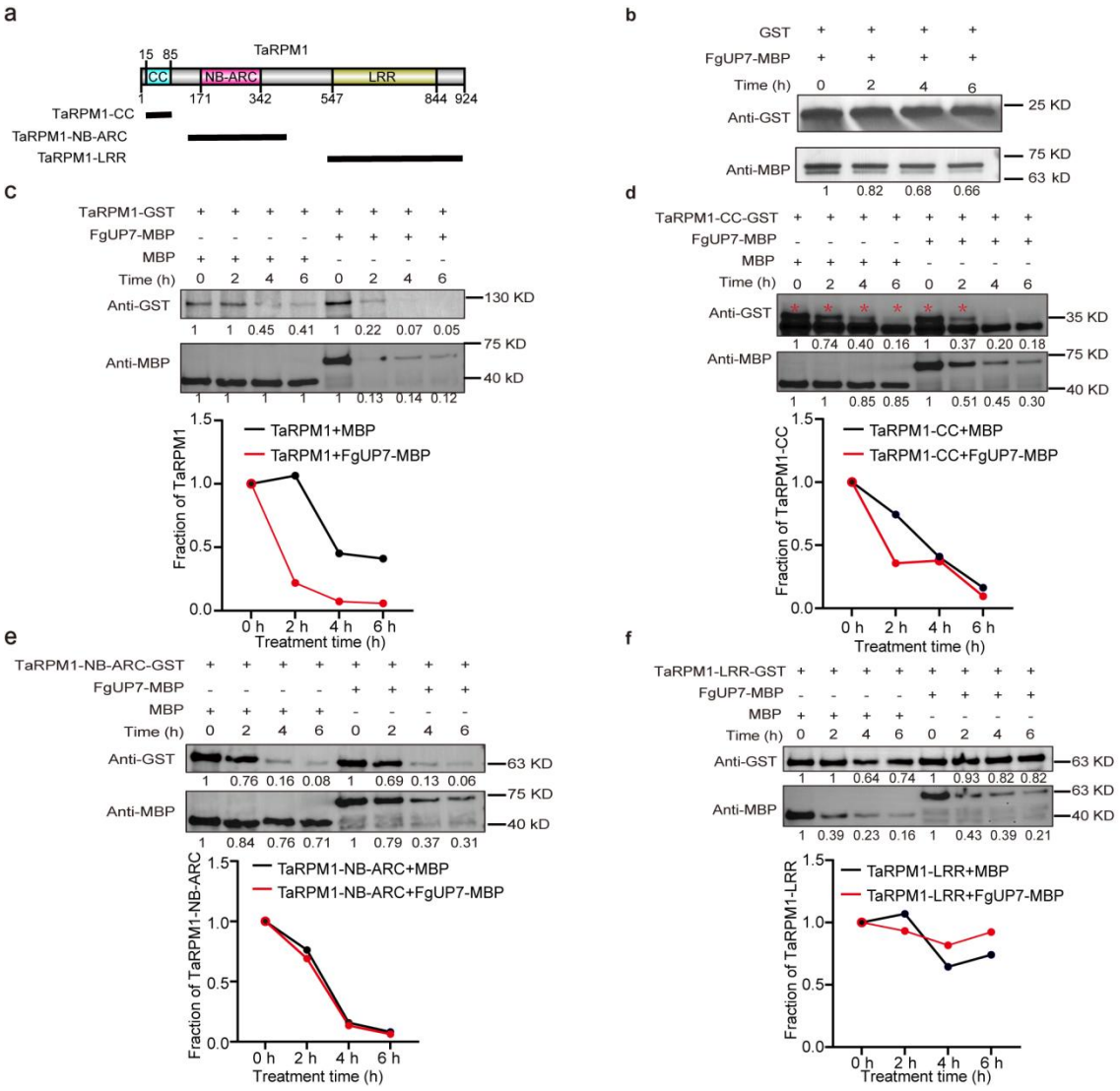

Supplementary Fig. 3 Schematic representation of TaRPM1 protein domain architecture and FgUP7-mediated degradation of TaRPM1.

(a) Diagram of TaRPM1 domain truncations.

(b-f) In vitro degradation assays examining the effect of FgUP7 on full-length TaRPM1 and its truncated proteins. MBP-FgUP7 was co-incubated with GST (**b**), GST-TaRPM1 (**c**), GST-TaRPM1-CC (**d**), GST-TaRPM1-NB-ARC (**e**), or GST-TaRPM1-LRR (**f**) at 37°C for 0, 2, 4, and 6 hours. Protein levels were detected using anti-MBP and anti-GST antibodies.

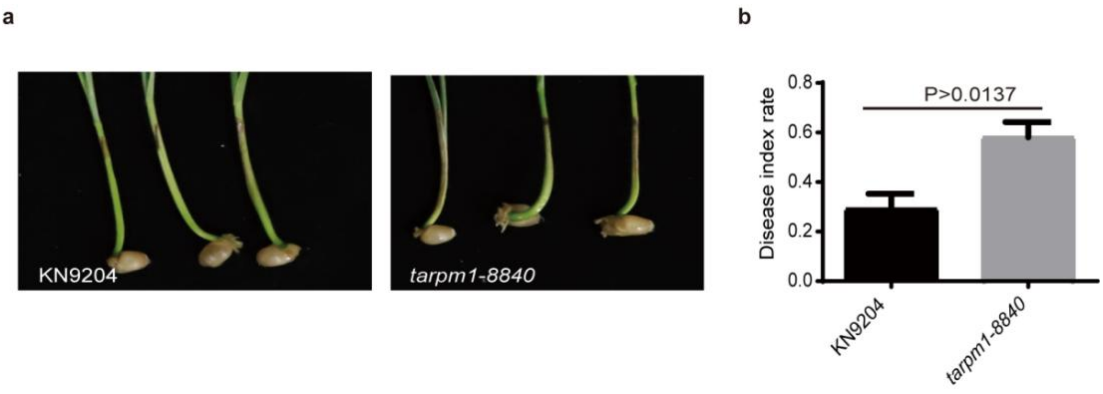

Supplementary Fig. 4 The KN9204 mutant of TaRPM1 confers susceptibility to *F. graminearum*.

(a) Disease symptoms on coleoptiles of the *knrpm1*-8840 mutant at 5 days post-inoculation with the wild-type *F. graminearum* strain.

(b) Distribution of disease indices on coleoptiles of the *knrpm1*-8840 mutant at 5 days post-inoculation with the wild-type *F. graminearum* strain. Data are from three independent experiments.

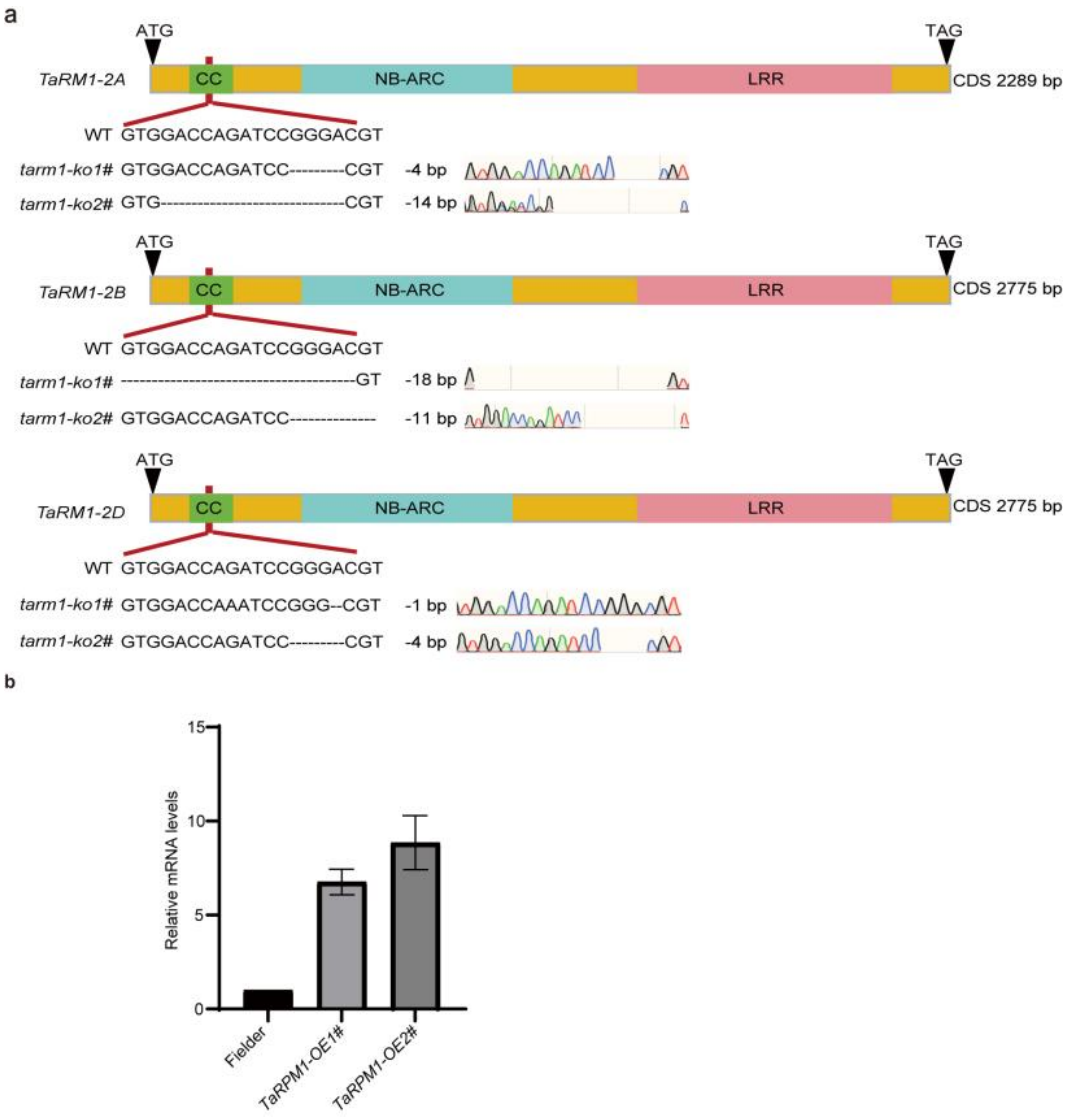

Supplementary Fig. 5 Editing types and expression levels of *TaRPM1* transgenics.

(a) CRISPR/Cas9-mediated gene editing of *TaRPM1*. Mutations of *TaRPM1* from individual editing lines (KO1#, KO2#) were confirmed by DNA sequencing and are presented as chromatographs. The number followed by chromatographs represents the nucleotide change (-, nucleotides missing).

(b) The expression levels in T3 generation *TaRPM1* overexpressing lines (OE1# and OE2#) were determined by RT–qPCR. Data represent mean ± s.e.m (n = 3).

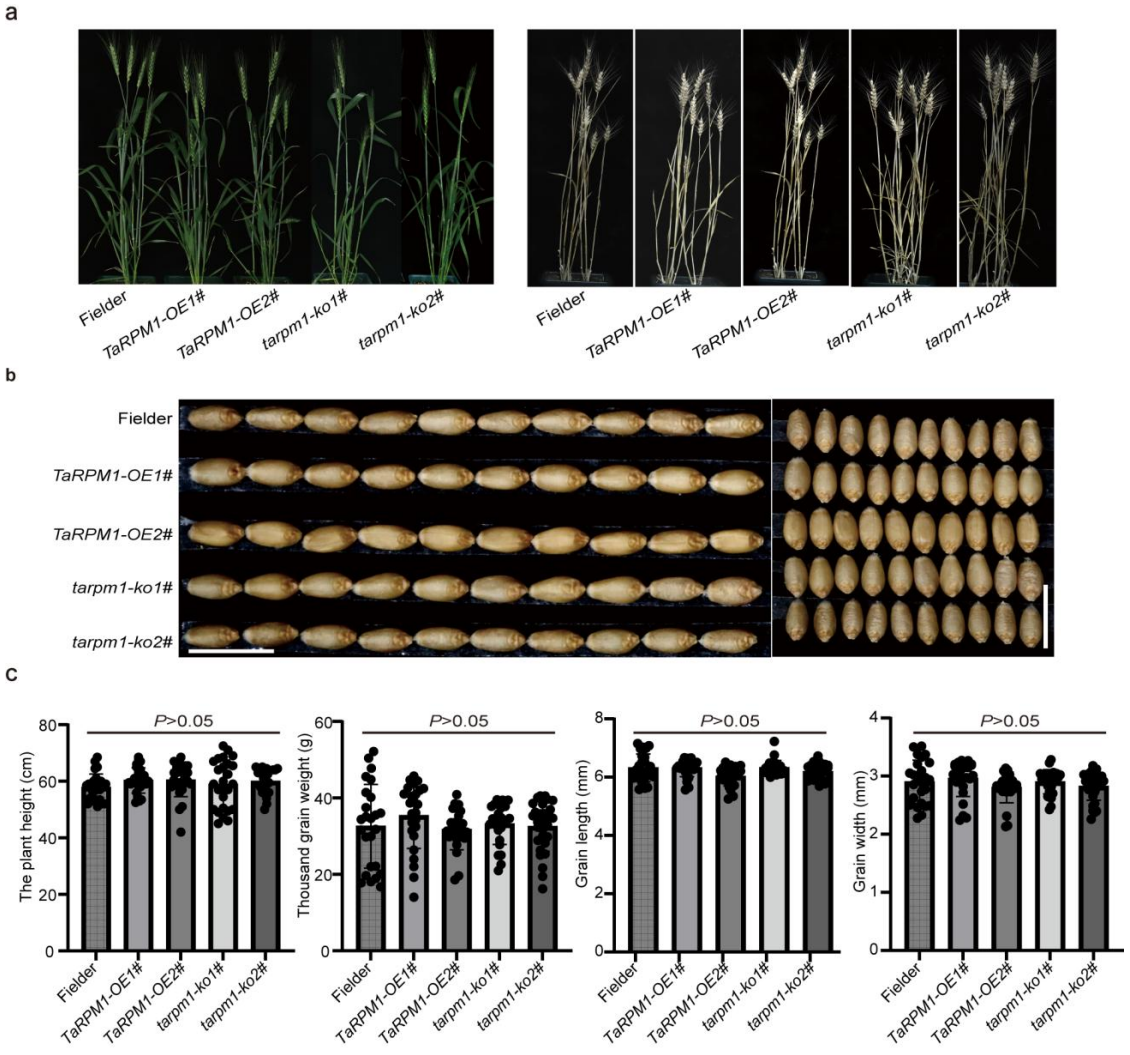

Supplementary Fig. 6 Overexpression of *TaRPM1* has no significant effect on the agronomic traits of wheat.

(a) Representative images of Fielder, *TaRPM1*-OE, and *TaRPM1*-KO plants at the flowering stage and mature stage.

(b) Seed shape of Fielder, *TaRPM1*-OE, and *TaRPM1*-KO plants at the kernel ripe stage. Bar, 1 cm. **c** Time to heading, plant height, thousand-grain, weight grain width, and grain length of Fielder, *TaRPM1*-OE, and *TaRPM1*-KO plants. Values represent the means ± SD from at least three independent replicates. All the data were compared to that of wild-type Fielder using a one-way ANOVA test. In the box plots: center line, median; box, interquartile range; whiskers, 1.5× interquartile range; and point, the data for agronomic traits.

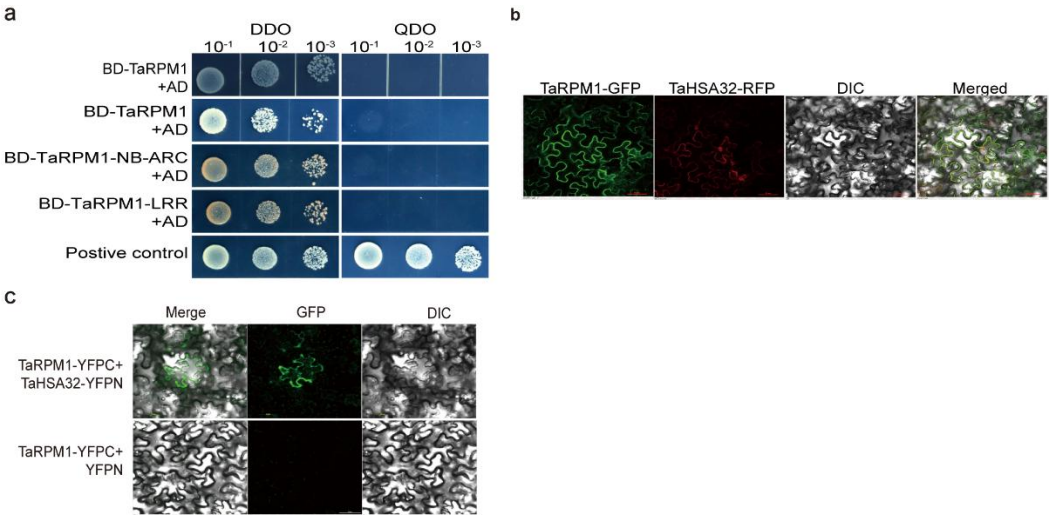

Supplementary Fig. 7 TaRPM1 interacts with TaHSA32.

(a) Yeast two-hybrid assays showed no interaction between the empty AD vector and TaRPM1 or its domains (CC, NB-ARC, LRR), confirming that these constructs serve as negative controls. Transformants were grown on DDO (SD/-Trp/-Leu) and QDO (SD/-Trp/-Leu/-His/-Ade) media.

(b) Co-localization of TaRPM1 and TaHSA32. *N. benthamiana* leaves were infiltrated with a mixture of *A. tumefaciens* strains co-expressing the indicated constructs. Fluorescence signals were detected at 48 hpi. Bar, 50 μm.

(c) Interaction between TaRPM1 and TaHSA32 was detected using BiFC assays. *N. benthamiana* leaves were infiltrated with a mixture of *A. tumefaciens* strains co-expressing indicated constructs. GFP signals were detected at 48 hpi. Bar, 50 μm.

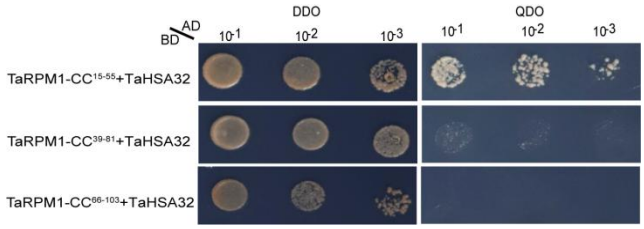

Supplementary Fig. 8 The N-terminus of TaRPM1-CC are required for interactions with TaHSA32.

Interaction assays of TaHSA32 with TaRPM1-CC mutants in yeast. Transformants were grown on DDO (SD/-Trp/-Leu) and QDO (SD/-Trp/-Leu/-His/-Ade) media.

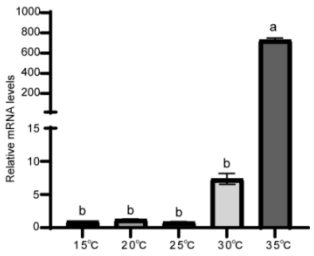

Supplementary Fig. 9 Temperature induction of TaHSA32.

RT–qPCR was performed to assess the transcript levels of *TaHSA32* in wheat leafs subjected to 6-hour treatments at different temperatures (15, 20, 25, 30, and 35 °C). *TaActin* was used as the internal reference gene. Values are mean ± SD (n=3). Different letters indicate significant differences ($P < 0.05$) based on one–way ANOVA and Duncan's multiple range test.

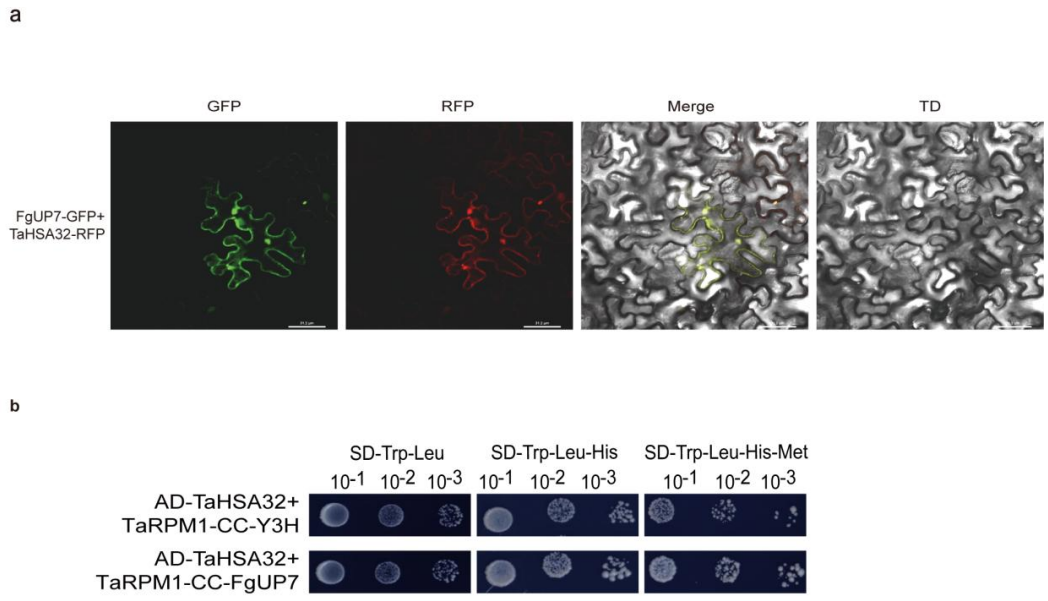

Supplementary Fig. 10 FgUP7 and TaHSA32 are co-localized.

(a) Co-localization of FgUP7 and TaHSA32 *N. benthamiana* leaves were infiltrated with a mixture of *A. tumefaciens* strains co-expressing the indicated constructs. Fluorescence signals were detected at 48 hpi. Bar, 50 μm.

(b) Yeast three-hybrid assay was performed to assess TaRPM1-CC-TaHSA32 interaction in the presence or absence of FgUP7. An unlabeled TaRPM1-CC construct was used as a control.

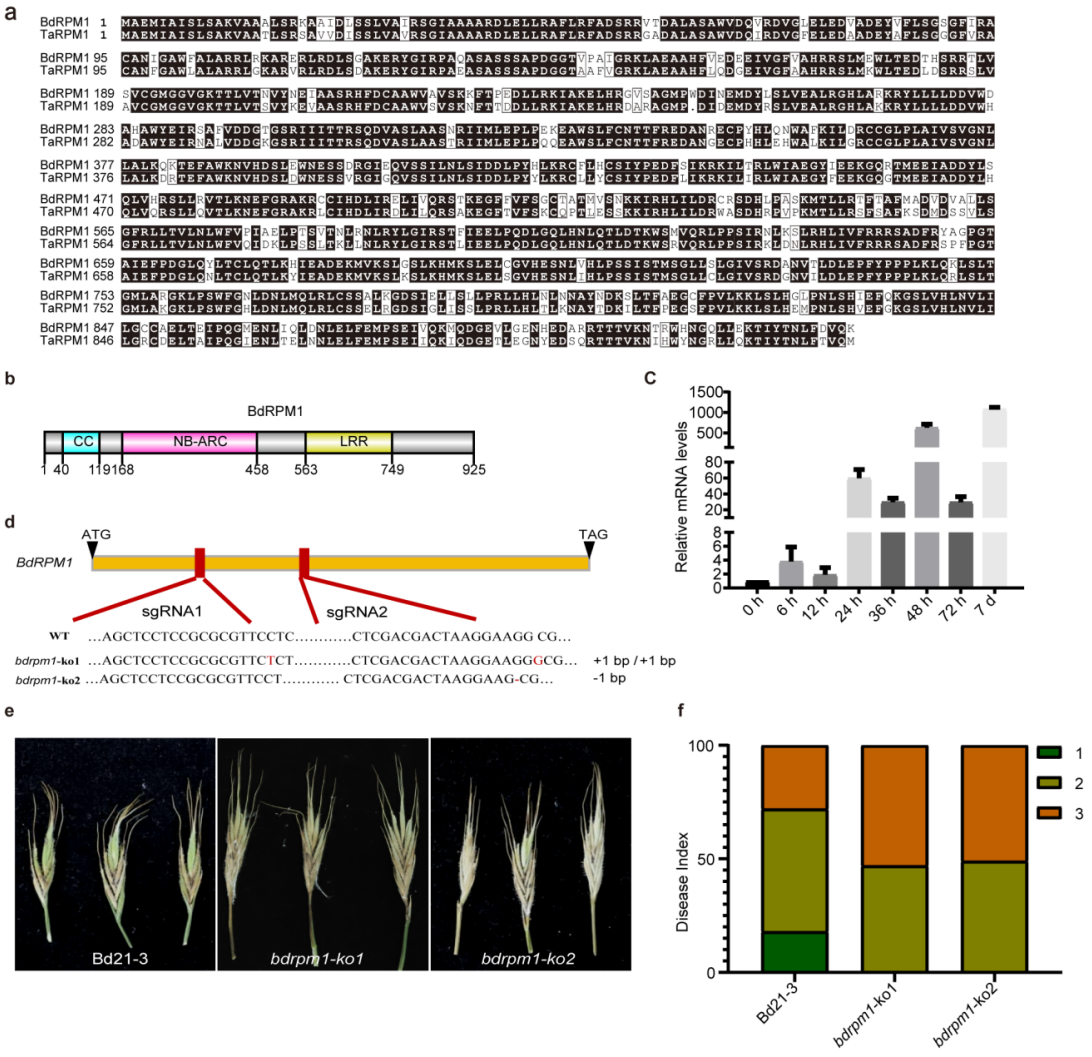

Supplementary Fig. 11 BdRPM1 positively regulates *B. distachyon* resistance to *F. graminearum*.

(a) Protein homology alignment between TaRPM1 and BdRPM1;

(b) Schematic diagram of the protein structure of BdRPM1;

(c) RT–qPCR analysis of BdRPM1 induction by *F. graminearum* infection. Expression levels were normalized to the non-inoculated spike tissues of Bd21-3 at 3 days (set as 1), with *BdTUA6* used as the internal reference gene. Data are from three biological replicates;

(d) CRISPR/Cas9-mediated gene editing of *BdRPM1*. Mutations in *BdRPM1* from individual edited lines (ko1, ko2) were confirmed by DNA sequencing. Numbers indicate

nucleotide changes (−, nucleotide deletion; +, nucleotide insertion). **e** Representative images of Bd21-3 and *bdrpm1*-ko spikes inoculated with the wild-type strain of *F. graminearum*, photographed at 7 days post-inoculation (dpi);

(f) Disease index distribution in Bd21-3 and *bdrpm1*-KO spikes at 10 dpi after inoculation with the wild-type strain of *F. graminearum*, determined from three independent experiments.

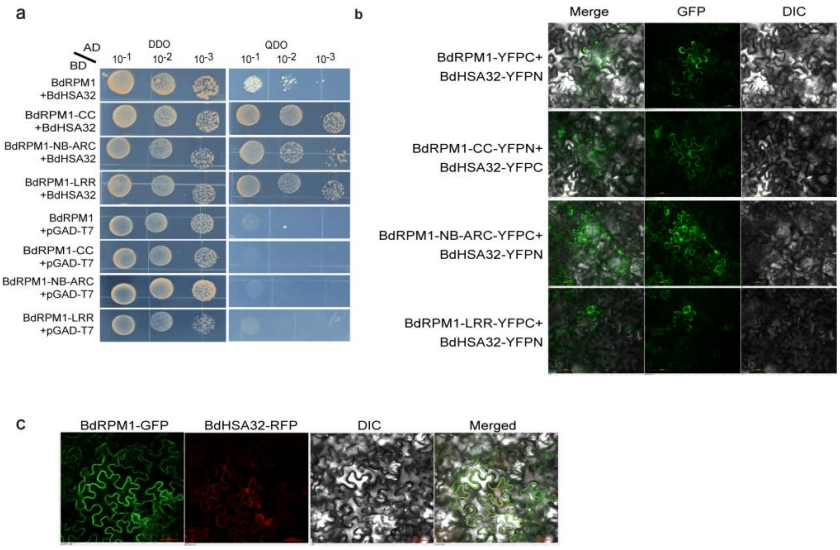

Supplementary Fig. 12 BdRPM1 interacts with BdHSA32.

(a) Yeast two-hybrid assays revealed an interaction between BdRPM1 (or its individual domains: CC, NB-ARC, and LRR) and BdHSA32. No interaction was observed between the empty AD vector and BdRPM1 or its domains (CC, NB-ARC, LRR), confirming that these domains served as negative controls. Transformants were cultured on DDO (SD/-Trp/-Leu) and QDO (SD/-Trp/-Leu/-His/-Ade) media.

(b) Interaction between BdRPM1 (and its truncations BdRPM1-CC, -NB-ARC, and -LRR) and BdHSA32 was detected using BiFC assays. *N. benthamiana* leaves were infiltrated with a mixture of *A. tumefaciens* strains co-expressing indicated constructs. GFP signals were detected at 48 hpi. Bar, 50 μm.

(c) Co-localization of BdRPM1 and BdHSA32. *N. benthamiana* leaves were infiltrated with a mixture of *A. tumefaciens* strains co-expressing the indicated constructs. Fluorescence signals were detected at 48 hpi. Bar, 50 μm.